Limitations of graphene nanocoated optical tapers for high-power nonlinear applications

Paul Mouchel, Meriem Kemel, Georges Semaan, Mohamed Salhi, Marc Le Flohic, François Sanchez

Limitations of graphene nanocoated optical tapers for high-power nonlinear applications

P. Mouchel[a,b,*], M. Kemel[a], G. Semaan[a], M. Salhi[a], M. Le Flohic[b], F. Sanchez[a]

[a] *Laboratoire de Photonique d'Angers, E. A. 4464, Université d'Angers, 2 bd Lavoisier, 49045 Angers, France*
[b] *Lumibird, 2 rue Paul Sabatier, 22300 Lannion, France*

Abstract

In this letter, we investigate the limitations of graphene as a saturable absorber for high-power nonlinear optical applications. The response of graphene nanocoated optical tapers against the average optical power injected is tested. We point out that the power handled by such components is limited and their nonlinear properties are strongly and permanently modified when exposed to high optical power. The origin of the degradation of the components is discussed.

Keywords: Graphene, optical tapers, nonlinear optics, mode-locking, fiber laser

1. Introduction

In the past decade, mode-locked fiber laser based on real saturable absorbers (SAs) have been widely used for producing ultrashort pulses. Graphene in particular has drawn the scientific community's attention as a remarkable SA. Multiple techniques for fabricating such passive components have been proposed. A nano-sheet of graphene can be trapped between two fiber connectors[1, 2, 3, 4, 5, 6] or collimators[7]. It can also be deposited as nano-flakes on a D-shaped side-polished fiber[8, 9], inside the air gaps of a photonic crystal fiber[10], or along the waist of a tapered fiber[11, 12, 13, 14, 15]. When inserted in the cavity of a fiber laser, graphene nanocoated optical tapers (GNOTs) were able to achieve mode-locking with an average power up to 520 mW and picosecond pulses.

In this article we investigate the deterioration of the characteristics of saturable absorption of nanocoated fiber tapers. The fabrication of the components is as described in reference [15]. The tapers' waist is 5-mm long and of diameter 20 µm. Graphene is in the form of multilayers nano-flakes in suspension

*Corresponding author
Email address: pmouchel@lumibird.com (P. Mouchel)

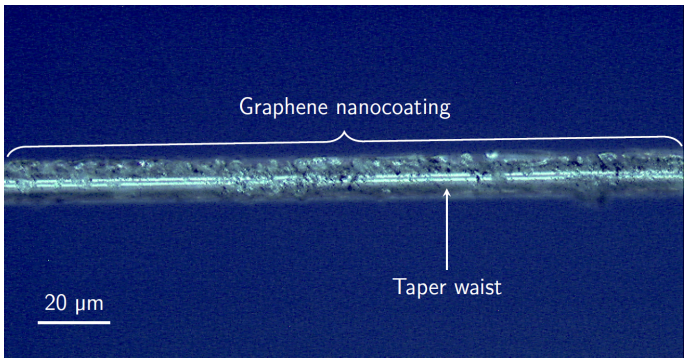

Figure 1: Deposition of graphene on the waist of a taper. The flakes are regularly deposited along the waist and form a coating.

in water ($1\,\mathrm{mg}\cdot\mathrm{ml}^{-1}$, Sigma-Aldrich 799092-50ML) and the deposition process is based on the optical tweezers effect. At the end of the process, the flakes of graphene form a coating around the waist of the taper and the beginning of the transitions as shown in figure 1.

2. Materials and methods

The nonlinear optical properties of the components are measured in a power-dependent setup described in figure 2. The source is a home-made pulsed laser centered at 1562 nm with a repetition rate of 12 MHz and a pulse width of 5 ps. A coupler spliced at the output of the laser splits the optical power in its two output fibers. One is spliced to the GNOT and the other stands as a reference. The power transmitted by both the reference fiber and the taper is measured by integrating spheres (Thorlabs S145C and S146C respectively). Different models have been proposed to fit the experimental transmission curves[1, 5, 16, 17, 18, 19]. However, each of them is adapted to only few situations. We propose here a more general formula allowing to accurately describe all the situations encountered in our work. The goal is to be able to compare the characteristics of a large number of samples. The evolution of the transmission T regarding the average input power P can be fitted by the equation

$$T(P) = 1 - \frac{\alpha_s}{1 + \left(\frac{P}{P_{sat}}\right)^n} - \alpha_{ns} \tag{1}$$

where α_s is the modulation depth of the transmission, α_{ns} is the non-saturable (linear) losses and P_{sat}, the saturation power, is such that $T(P_{sat})$ corresponds to an augmentation of half the modulation depth. In contrast to previous models, the free parameter n has been introduced to allow a better fitting of the switching region. It controls the steepness of the slope.

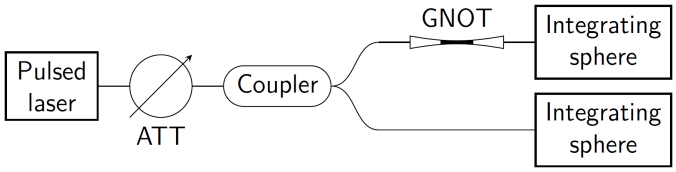

Figure 2: Schematics of the power-dependent setup. ATT: variable attenuator. GNOT: graphene nanocoated optical taper.

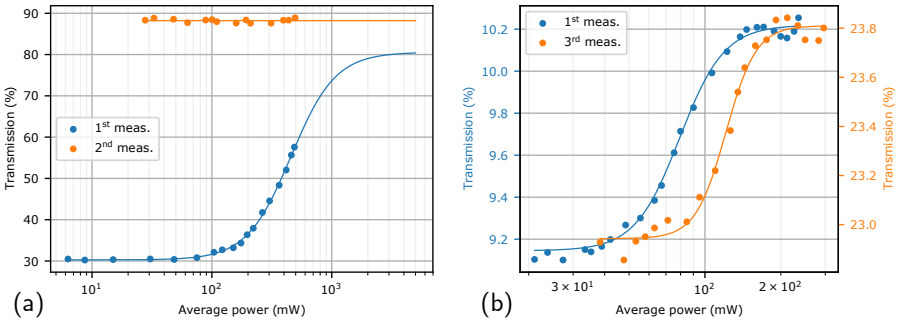

Figure 3: Evolution of the transmission of two GNOTs following consecutive characterizations. The dots represent the values measured and the lines are the fitted curves following Eq. (1). (a) After the second measurement, the component has lost its nonlinear properties. (b) After the third measurement, the saturation power has increased and the linear losses have been reduced.

3. Results and discussion

Various GNOTs were characterized using this method. From these measurements, three different behaviors were observed. The normal and expected behavior is a repeatability of both the SA properties and the fit parameters obtained over successive measurements. This first behavior is the normal one for a functioning component which has good stability and reproducibility. Surprisingly, we also observed modifications of the characteristics of saturable absorption from consecutive measurements. Indeed, the GNOT can either lose its nonlinear properties or undergo a significant modification of the fitting parameters thus revealing a possible optical damage of the components. Experimental demonstration is given in figure 3 which presents the transmission of two GNOTs whose characteristics are typical examples of the degradation of the performances of the components.

Figure 3a presents the characterization of the first taper right after the deposition. The first measurement is limited by the maximum average power available with the setup used. The saturated transmission cannot be plotted. The measurement is fitted by equation (1). The modulation depth is 50 %, the saturation power is 460 mW and the free parameter n is 2.4. The fit predicts 20 % of linear losses. At the end of the measurement, up to 500 mW were

injected in the GNOT and its transmission was 57 %. The second measurement shows that the taper has a nearly constant transmission of 88 %. It is independent of the incident power. In figure 3b, the characteristics of a second GNOT's saturable absorption evolved from three consecutive measurements. From the first to the last test, the saturation power increased from 79 mW to 121 mW, the non-saturable absorption decreased from 90 % to 76 % and the parameter n increased from 4.9 to 7.2. The modulation depth was stable around 1 %. For a better readability of the graph, the scale of the y-axis is different for the first and third measurements.

The power-dependent setup was tested by a taper with no graphene deposited on the waist and with similar geometrical properties. The transmission of the taper is stable over time (tested for 20 minutes) and at different incident average powers (up to 600 mW). The variation around the average measured transmission is less than 1 %. The transmission of the coupler was also tested with a variation of 0.1 %. From these tests, we can confidently conclude that the differences in saturable absorption described previously come from the graphene deposited.

Most of the tapers whose characteristics were stable from consecutive measurements had a small saturation power (around 10 mW) and were not exposed to high power during the process. In order to determine if the incident power plays a role in the deterioration of the components, the stability of transmission of a GNOT over time is measured at different incident powers. The setup is the same as the one used for characterizing the components. The laser emits 5 ps pulses at a central wavelength of 1562 nm and its average power is controlled by a variable attenuator spliced at the output. Six measurements are made consecutively on the same component between 10 mW and 166 mW. At each pump level, the transmission is measured every second for 20 minutes. The input power is then increased and the stability is measured again. Figure 4 presents the results of this test. For an incident mean power less than 100 mW, the transmission of the GNOT is relatively stable around 38.5 %. Then, for higher input power, we observe an increase in the transmission over time. This process is irreversible. By repeating this process on three more GNOTs, the damage threshold was determined to be around 150 mW of average incident power.

We assume that the changes in transmission are the consequence of a degradation of the graphene nano-flakes deposited on the taper. Following the absorption of a photon, graphene generates heat and relaxes rapidly[20]. In our experiment, the GNOT is fixed in a glass mount and air is surrounding the fiber. There is no active method of cooling the component. Due to the low thermal conductivity of air ($0.026\,\mathrm{W}\cdot\mathrm{m}^{-1}\cdot\mathrm{K}^{-1}$ at 25 °C[21]), the component generates more heat than it is capable of dissipating. The temperature of the components was measured with a thermal camera (Chauvin Arnoux C.A 1882 DiaCAm) at different incident powers. Figure 5 presents the evolution of the temperature of the GNOT for average powers between 10 mW and 400 mW. Below the threshold of 150 mW, the temperature increases up to 124 °C. Above the threshold, the temperature continues to rise before stabilizing around 180 °C. It is impor-

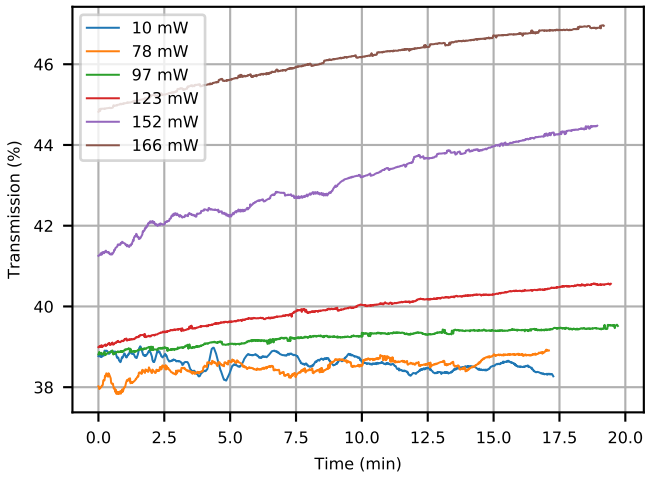

Figure 4: Evolution of the transmission of a GNOT over time for different incident average powers.

tant to note that because of both the size of the taper and the low resolution of the thermal camera, the area of interest was only seen by an array of about 50×4 pixels. The temperature measured was most likely averaged over the surface represented by a pixel and the peak temperature of the component is certainly higher than the ones presented in Fig. 5.

It has been showed that defects appear on the edges of the crystal structure of flakes of graphene when their temperature reaches 200 °C and in the center of the flakes for temperatures up to 500 °C[22, 23, 24]. As flakes are deposited randomly on the surface of the waist and interact with the evanescent field of clad modes propagating in the taper, the absorption takes part mostly on the edges. At low temperature (and incident power), graphene behaves normally as the structure of the flakes is not disrupted by the heat. When the temperature increases further, defects appear and the flakes stop absorbing incident optical power. In the case of a modification of the saturable absorption parameters of the GNOT (Fig. 3b), only a fraction of the flakes is impacted by the heat. If most flakes are affected, the GNOT loses its nonlinear properties (Fig. 3a). An analysis of the graphene deposited on a defective GNOT by Raman spectroscopy would give further information but we did not have access to such technology during the study. Moreover, the nanocoating of defective components presented no visible damage and the nano-flakes were still surrounding the waist of the taper, implying that the modification of absorption of the component is not a result of the disbonding of graphene from the taper but rather a structural modification of graphene.

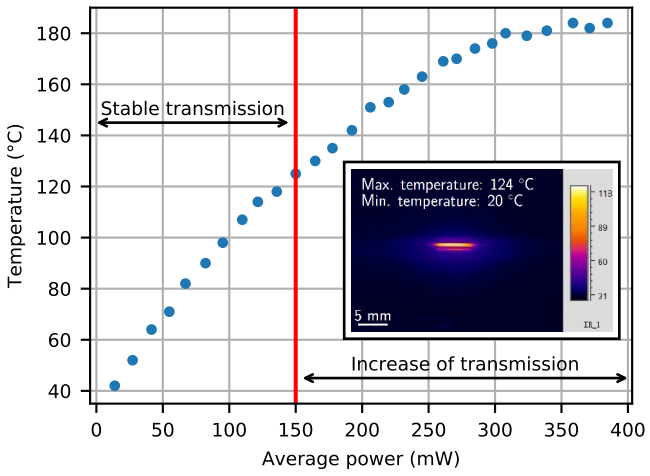

Figure 5: Evolution of the temperature of a GNOT for different incident average powers. Inset: infrared image of the GNOT when the incident average power is 150 mW.

4. Conclusion

In conclusion, we have demonstrated the limitations of real saturable absorbers based on graphene nano-flakes deposited on the waist of a taper. At low incident average power, the components behave normally but when the incident power is higher than a threshold (determined around 150 mW), they lose their nonlinear characteristics. The origin of the instability is a degradation of the graphene nano-flakes caused by an excessive amount of heat badly dissipated. For a use of such a component for high power mode-locking, the taper will need to be correctly cooled. For instance, it could be surrounded by a material with great heat conductivity and optical properties in compliance with the propagation of clad modes (low refractive index and transparent in the infrared). We expect that similar damage on the nonlinear properties of graphene could occur more generally in any graphene-based optical component subjected to power levels of few hundreds of milliwatts. Graphene is widely used for its nonlinear optical properties and these results could potentially impact all applications based on such properties.

Funding

This work was supported by Lumibird and the ANRT (Association Nationale de la Recherche et de la Technologie) under the doctoral CIFRE (Convention Industrielle de Formation par la Recherche) contract of Mr. Paul Mouchel.

References

[1] Q. Bao, H. Zhang, Y. Wang, Z. Ni, Y. Yan, Z. X. Shen, K. P. Loh, D. Y. Tang, Atomic-layer graphene as a saturable absorber for ultrafast pulsed lasers, Advanced Functional Materials 19 (19) (2009) 3077–3083. doi:10.1002/adfm.200901007.

[2] H. Zhang, D. Y. Tang, L. Zhao, Q. Bao, K. P. Loh, Large energy mode locking of an erbium-doped fiber laser with atomic layer graphene, Optics Express 17 (20) (2009) 17630–17635. doi:10.1364/OE.17.017630.

[3] Z. Sun, T. Hasan, F. Torrisi, D. Popa, G. Privitera, F. Wang, F. Bonaccorso, D. M. Basko, A. C. Ferrari, Graphene mode-locked ultrafast laser, ACS Nano 4 (2) (2010) 803–810. doi:10.1021/nn901703e.

[4] Y. Meng, S. Zhang, X. Li, H. Li, J. Du, Y. Hao, Multiple-soliton dynamic patterns in a graphene mode-locked fiber laser, Optics express 20 (6) (2012) 6685–6692. doi:10.1364/OE.20.006685.

[5] G. Sobon, J. Sotor, K. M. Abramski, Passive harmonic mode-locking in Er-doped fiber laser based on graphene saturable absorber with repetition rates scalable to 2.22 GHz, Applied Physics Letters 100 (16) (2012) 161109. doi:10.1063/1.4704913.

[6] Y. Meng, A. Niang, K. Guesmi, M. Salhi, F. Sanchez, 1.61 µm high-order passive harmonic mode locking in a fiber laser based on graphene saturable absorber, Optics Express 22 (24) (2014) 29921. doi:10.1364/OE.22.029921.

[7] Z.-C. Luo, W.-J. Cao, A.-P. Luo, W.-C. Xu, Optical deposition of graphene saturable absorber integrated in a fiber laser using a slot collimator for passive mode-locking, Applied Physics Express 5 (5) (2012) 055103. doi:10.1143/APEX.5.055103.

[8] T. Chen, C. Liao, D. N. Wang, Y. Wang, Passively mode-locked fiber laser by using monolayer chemical vapor deposition of graphene on D-shaped fiber, Applied Optics 53 (13) (2014) 2828. doi:10.1364/AO.53.002828.

[9] J. D. Zapata, D. Steinberg, L. A. M. Saito, R. E. P. de Oliveira, A. M. Càrdenas, E. A. T. de Souza, Efficient graphene saturable absorbers on D-shaped optical fiber for ultrashort pulse generation, Scientific Reports 6 (1) (2016) 20644. doi:10.1038/srep20644.

[10] J. Zhao, S. Ruan, P. Yan, H. Zhang, Y. Yu, H. Wei, J. Luo, Cladding-filled graphene in a photonic crystal fiber as a saturable absorber and its first application for ultrafast all-fiber laser, Optical Engineering 52 (10) (2013) 106105. doi:10.1117/1.OE.52.10.106105.

[11] J. Wang, Z. Luo, M. Zhou, C. Ye, H. Fu, Z. Cai, H. Cheng, H. Xu, W. Qi, Evanescent-light deposition of graphene onto tapered fibers for passive Q-switch and mode-locker, IEEE Photonics Journal 4 (5) (2012) 1295–1305. doi:10.1109/JPHOT.2012.2208736.

[12] N. Zhao, M. Liu, H. Liu, X.-W. Zheng, Q.-Y. Ning, A.-P. Luo, Z.-C. Luo, W.-C. Xu, Dual-wavelength rectangular pulse Yb-doped fiber laser using a microfiber-based graphene saturable absorber, Optics Express 22 (9) (2014) 10906. doi:10.1364/OE.22.010906.

[13] T. Chen, H. Chen, D. N. Wang, Graphene saturable absorber based on slightly tapered fiber with inner air-cavity, Journal of Lightwave Technology 33 (11) (2015) 2332–2336. doi:10.1109/JLT.2015.2410912.

[14] X. M. Liu, H. R. Yang, Y. D. Cui, G. W. Chen, Y. Yang, X. Q. Wu, X. K. Yao, D. D. Han, X. X. Han, C. Zeng, J. Guo, W. L. Li, G. Cheng, L. M. Tong, Graphene-clad microfibre saturable absorber for ultrafast fibre lasers, Scientific Reports 6 (1) (2016) 26024. doi:10.1038/srep26024.

[15] P. Mouchel, G. Semaan, A. Niang, M. Salhi, M. Le Flohic, F. Sanchez, High power passively mode-locked fiber laser based on graphene nanocoated optical taper, Applied Physics Letters 111 (3) (2017) 031106. doi:10.1063/1.4994026.

[16] Z. Wang, H. Mu, C. Zhao, Q. Bao, H. Zhang, Harmonic mode-locking and wavelength-tunable Q-switching operation in the graphene-Bi_2Te_3 heterostructure saturable absorber-based fiber laser, Optical Engineering 55 (8) (2016) 081314. doi:10.1117/1.OE.55.8.081314.

[17] T. Schibli, E. Thoen, F. Kärtner, E. Ippen, Suppression of Q-switched mode locking and break-up into multiple pulses by inverse saturable absorption, Applied Physics B 70 (S1) (2000) S41–S49. doi:10.1007/s003400000331.

[18] C. A. Zaugg, Z. Sun, V. J. Wittwer, D. Popa, S. Milana, T. S. Kulmala, R. S. Sundaram, M. Mangold, O. D. Sieber, M. Golling, Y. Lee, J. H. Ahn, A. C. Ferrari, U. Keller, Ultrafast and widely tuneable vertical-external-cavity surface-emitting laser, mode-locked by a graphene-integrated distributed Bragg reflector, Optics Express 21 (25) (2013) 31548. doi:10.1364/OE.21.031548.

[19] A. Marini, J. D. Cox, F. J. García de Abajo, Theory of graphene saturable absorption, Physical Review B 95 (12) (2017) 125408. doi:10.1103/PhysRevB.95.125408.

[20] G. Xing, H. Guo, X. Zhang, T. C. Sum, C. H. A. Huan, The physics of ultrafast saturable absorption in graphene, Optics Express 18 (5) (2010) 4564. doi:10.1364/OE.18.004564.

[21] E. W. Lemmon, R. T. Jacobsen, Viscosity and thermal conductivity equations for nitrogen, oxygen, argon, and air, International Journal of Thermophysics 25 (1) (2004) 21–69. doi:10.1023/B:IJOT.0000022327.04529.f3.

[22] Y. N. Xu, D. Zhan, L. Liu, H. Suo, Z. H. Ni, T. T. Nguyen, C. Zhao, Z. X. Shen, Thermal dynamics of graphene edges investigated by polarized Raman spectroscopy, ACS Nano 5 (1) (2011) 147–152. doi:10.1021/nn101920c.

[23] H. Y. Nan, Z. H. Ni, J. Wang, Z. Zafar, Z. X. Shi, Y. Y. Wang, The thermal stability of graphene in air investigated by Raman spectroscopy, Journal of Raman Spectroscopy 44 (7) (2013) 1018–1021. doi:10.1002/jrs.4312.

[24] Y. Sun, M. Yanagisawa, T. Homma, Thermal stability of single-layer graphene subjected to confocal laser heating investigated by using in situ anti-Stokes and Stokes Raman spectroscopy, Electrochemistry 85 (4) (2017) 195–198. doi:10.5796/electrochemistry.85.195.

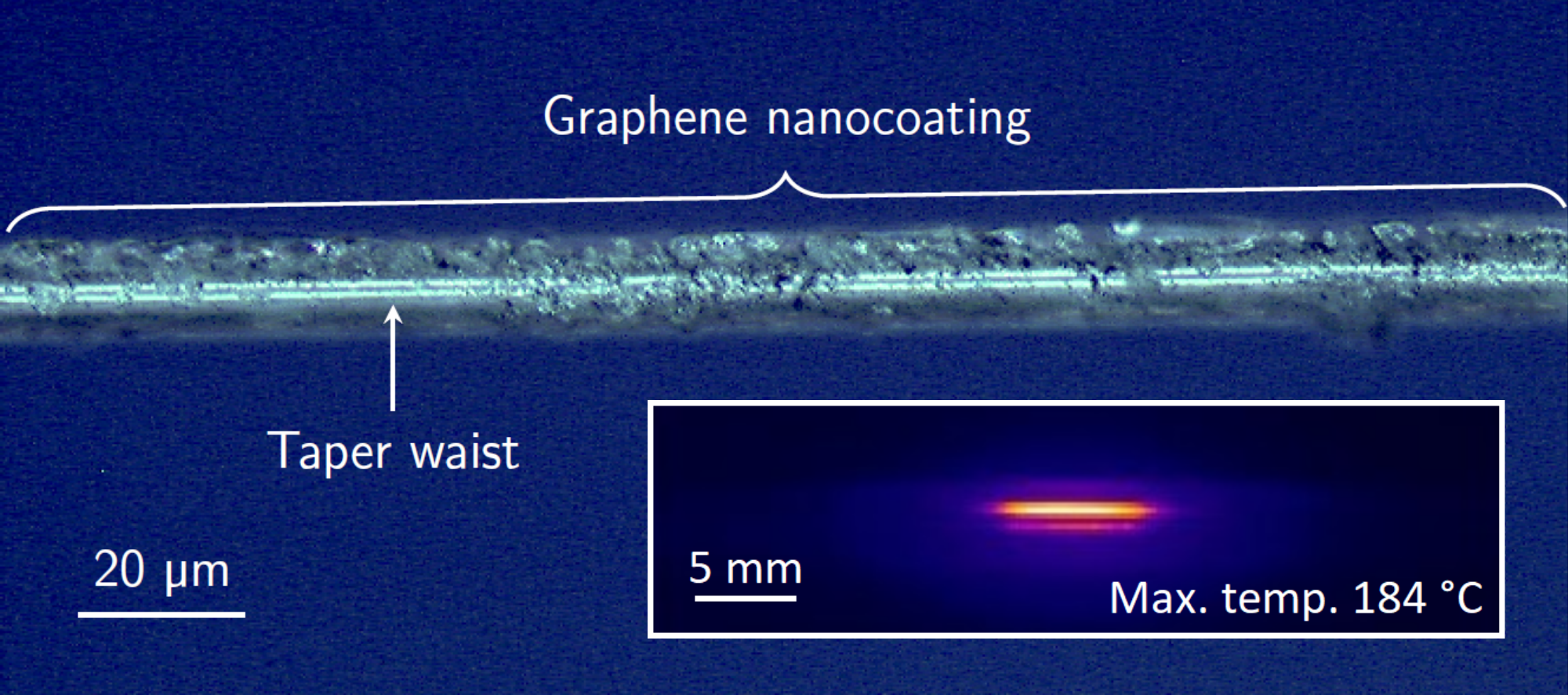
Graphene nanocoating
Taper waist
20 μm
5 mm
Max. temp. 184 °C